DOI: 10.1002/ejic.200701186

Reactions of Pyridyl Side Chain Functionalized Indenes with $Ru_3(CO)_{12}$

Dafa Chen,[a] Shansheng Xu,[a] Haibin Song,[a] and Baiquan Wang*[a,b]

Keywords: Ruthenium / Carbonyl ligands / C–H activation / Coordination modes / Arene ligands / Cluster compounds

Reactions of the pyridyl side chain functionalized indenes 3-R-C_9H_7 [R = $(C_5H_4N)CH_2CMe_2$ (**1**), $(MeC_5H_3N)CH_2CMe_2$ (**2**), $(C_5H_4N)CH_2$ (**6**)] with $Ru_3(CO)_{12}$ in refluxing xylene gave the facial coordinated indenyl cluster [μ_3-η^5:η^2:η^2-$(C_5H_3N)CH_2Me_2C(C_9H_6)$]$Ru_4(\mu_3\text{-}CO)(CO)_7$ (**8**), the *syn*-η^5:η^6-coordinated indenyl cluster [μ-η^5:η^6-$(MeC_5H_3N)CH_2CMe_2(C_9H_6)$]$Ru_2(CO)_3]_2$ (**10**), and the η^1:η^2-coordinated indenyl complex [η^2-$(C_5H_3N)CH_2(C_9H_7)$][η^1:η^2-$(C_5H_4N)CH_2(C_9H_6)$]$Ru_2(CO)_4$ (**18**), respectively, in addition to the normal diruthenium complexes [(η^5-RC_9H_6)Ru(CO)]$_2$(μ-CO)$_2$ [R = $(C_5H_4N)CH_2CMe_2$ (**7**), $(MeC_5H_3N)CH_2CMe_2$ (**9**), $(C_5H_4N)CH_2$ (**17**)]. When the pyridyl side chains were replaced by other bulky groups [R = *t*Bu (**3**), $PhCH_2Me_2C$ (**4**), $(C_9H_6N)CH_2Me_2C$ (**5**)], the similar *syn*-η^5:η^6-coordinated indenyl clusters **12**, **14**, and **16** were also obtained. When **1** or **2** were treated with $Ru_3(CO)_{12}$ in refluxing heptane, the ionic clusters {[$(C_5H_4N)CH_2Me_2C(C_9H_6)$]Ru$(CO)_2$}$^+$[$HRu_6(CO)_{18}$]$^-$ (**19**), [$(C_5H_4N)CH_2Me_2C(C_9H_8)$]$^+$[$HRu_6(CO)_{18}$]$^-$ (**20**), and complex **8** or ionic clusters {[$(MeC_5H_3N)CH_2Me_2C(C_9H_6)$]Ru$(CO)_2$}$^+$[$HRu_6(CO)_{18}$]$^-$ (**21**) and [$(MeC_5H_3N)CH_2Me_2C(C_9H_8)$]$^+$[$HRu_6(CO)_{18}$]$^-$ (**22**) were obtained. Similar treatment of **5** or **6** with $Ru_3(CO)_{12}$ in refluxing heptane gave the ionic clusters [$(C_9H_6N)CH_2Me_2C(C_9H_8)$]$^+$[$HRu_6(CO)_{18}$]$^-$ (**23**) or {[η^3-$(C_5H_4N)CH(C_9H_7)$][η^2-$(C_5H_4N)CH_2(C_9H_7)$]Ru(CO)}$^+$[$HRu_6(CO)_{18}$]$^-$ (**24**), respectively, in addition to complex **18** in the latter case. The molecular structures of **8**, **9**, **10**, **14**, **17**, **18**, **21**, **22**, and **24** were determined by X-ray diffraction analysis.

Introduction

Indenyl metal complexes have received increasing attention due to the diverse and flexible hapticities and the enhanced reactivities both in stoichiometric reactions and catalysis;[1] this is sometimes referred to as the *indenyl effect*.[2] More than 10 coordination modes have been found for the indenyl ligand.[3–6] The donor side chain functionalized cyclopentadienyl or indenyl ligands have usually been used to form intramolecular coordination to a Lewis acidic metal center or to construct oligonuclear metal complexes, which usually show different structures and reactivities.[7] In our previous work, we studied the reactions of pyridyl side chain functionalized cyclopentadienes with metal carbonyl and obtained some novel intramolecular C–H activated products.[8] By considering the various coordination modes between the indenyl group and the metal atoms, we further studied the reactions of pyridyl side chain functionalized indenes with $Ru_3(CO)_{12}$, and a series of indenyl ruthenium complexes with different coordination modes were obtained.

[a] State Key Laboratory of Elemento-Organic Chemistry, College of Chemistry, Nankai University,
Tianjin 300071, People's Republic of China
Fax: +86-22-23504781
E-mail: bqwang@nankai.edu.cn
[b] Key Laboratory of Organometallic Chemistry, Shanghai Institute of Organic Chemistry, Chinese Academy of Sciences, Shanghai 200032, People's Republic of China

Results and Discussion

Reaction of 1 with $Ru_3(CO)_{12}$ in Xylene

When **1**[9] was treated with $Ru_3(CO)_{12}$ in refluxing xylene for 5 h, the α-C–H bond of the pyridyl group activated product **8** was obtained in 29% yield, in addition to the normal diruthenium complex **7** (14%) (Scheme 1). Although xylene was used as the solvent, no product resulting from the reaction of $Ru_3(CO)_{12}$ with xylene was detected.[10] The lower yields can be attributed to the significant decomposition of $Ru_3(CO)_{12}$, which resulted in a large amount of dark solid that was not soluble in common solvents.

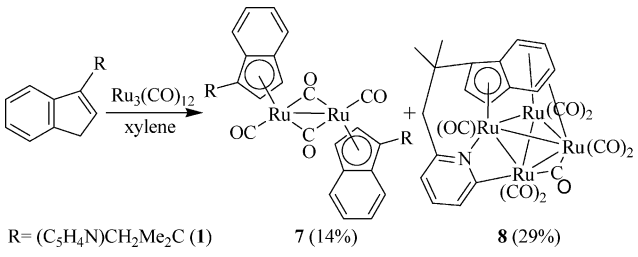

Scheme 1.

The IR spectrum of **7** shows terminal and bridging carbonyl group absorptions at 1957 and 1770 cm^{-1}, which is indicative of the symmetrical structure (*trans*). The IR spectrum of **8** shows eight carbonyl group absorptions at 2034–1851 cm^{-1}. Single-crystal X-ray diffraction analysis showed that complex **8** is an indenyl tetranuclear ruthenium cluster

(Figure 1). There are two crystallographically independent molecules, **8A** and **8B**, in the unit cell. In both of the two molecules, the metal framework consists of a tetrahedron with the indenyl group lying over one of the triangular faces in η^5:η^2:η^2 modes. The η^5-indenyl-coordinated Ru(3) or Ru(7) center is coordinated to the N atom of the pyridyl group. The Ru(4) or Ru(8) is bonded with the α-C of the pyridyl unit through C–H activation. Each of the indenyl ligands donates a total of 9 electrons, so the valence electrons of **8** are 62, which is in accord with the theoretical value.[11] There is a μ_3-CO ligand [C(14)–O(14)] that is asymmetrically bonding with Ru(5), Ru(6), and Ru(8) [Ru–C: 2.086(5), 2.464(6), 2.162(5) Å, respectively] in **8B**, and a μ-CO [C(6)–O(6)] ligand that bridges Ru(1) and Ru(4) in **8A**. The distances of Ru(6)–C(37) [2.238(4) Å], Ru(6)–C(38) [2.238(4) Å], Ru(2)–C(19) [2.199(5) Å], and Ru(2)–C(20) [2.245(5) Å] are similar, which supports the η^2 coordination mode. However, the distances of Ru(5)–C(36) [2.462(4) Å] and Ru(1)–C(18) [2.608 Å] are much longer than those of Ru(6)–C(35) [2.205(5) Å] and Ru(1)–C(17) [2.162(5) Å], which provides evidence for the twisted η^2 coordination. The Ru(1)–C(18) distance is even longer than those of Ru(2)–C(18) [2.467(5) Å], which is close to η^1:η^3 coordination. It agrees with the shorter distance of C(18)–C(19) [1.412(8) Å] than those of C(17)–C(18) [1.435(7) Å]. The greatly twisted η^2:η^2 coordination might be due to packing effects. Although there are two isomers in the unit cell, the ^{1}H NMR spectrum of **8** shows the existence of only one isomer. This indicates that they may exist as one form in solution; however, the fact that a rapid fluxional process exists cannot be excluded.[3c,12] Only a few complexes with μ_3-η^5:η^2:η^2-bonding indenyl ligands have been reported for ruthenium and osmium clusters,[5] so complex **8** is another example of this kind of complex.

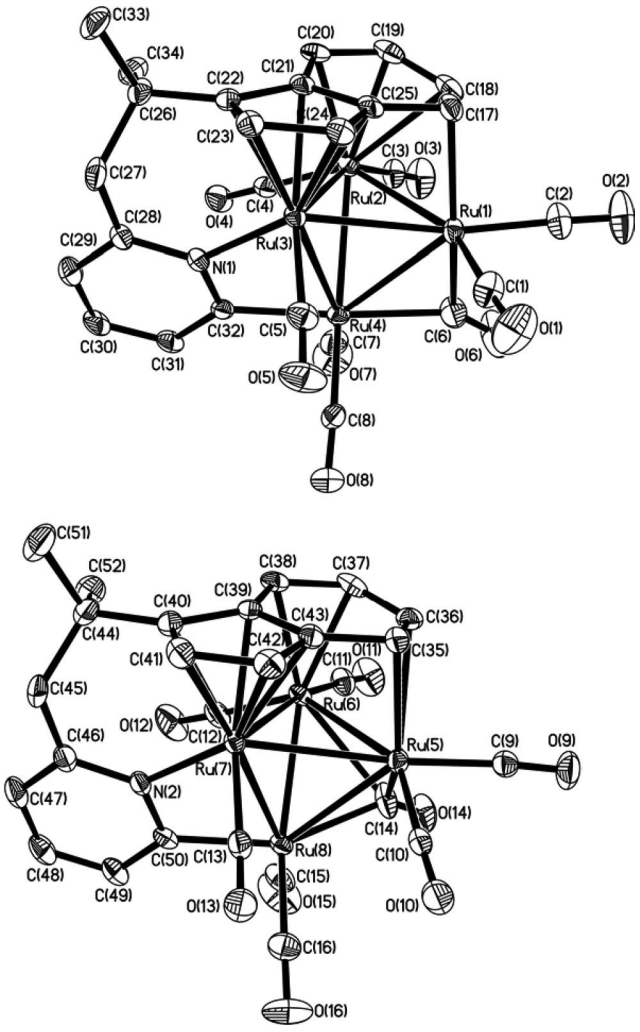

Figure 1. Molecular structure of **8**. Two crystallographically independent molecules in the unit cell are shown as **8A** (top) and (**8B**) (bottom). Selected bond lengths [Å]: Ru(1)–Ru(4) 2.7520(13), Ru(1)–Ru(3) 2.8074(16), Ru(1)–Ru(2) 2.8213(13), Ru(2)–Ru(4) 2.7568(14), Ru(2)–Ru(3) 2.9303(12), Ru(3)–Ru(4) 2.7492(13), Ru(1)–C(17) 2.162(5), Ru(2)–C(18) 2.467(5), Ru(2)–C(19) 2.199(5), Ru(2)–C(20) 2.245(5), Ru(3)–N(1) 2.098(4), Ru(4)–C(32) 2.062(4), Ru(5)–C(35) 2.205(5), Ru(5)–C(36) 2.462(4), Ru(5)–C(14) 2.086(5), Ru(6)–C(14) 2.464(6), Ru(6)–C(37) 2.238(4), Ru(6)–C(38) 2.238(4), Ru(8)–C(14) 2.162(5), Ru(8)–C(50) 2.052(5), Ru(7)–N(2) 2.097(4), C(17)–C(18) 1.435(7), C(17)–C(25) 1.444(6), C(18)–C(19) 1.412(8), C(19)–C(20) 1.396(7), C(20)–C(21) 1.435(6), C(21)–C(25) 1.466(6), C(35)–C(36) 1.408(7), C(35)–C(43) 1.455(6), C(36)–C(37) 1.420(7), C(37)–C(38) 1.399(7), C(38)–C(39) 1.443(6), C(39)–C(43) 1.465(6).

Considering the similarity of iron with ruthenium, the reaction of **1** with $Fe(CO)_5$ was also done but TLC analysis showed no product except for the decomposition of $Fe(CO)_5$, possibly due to the poor reactivity of $Fe(CO)_5$.

Reactions of 2–5 with $Ru_3(CO)_{12}$ in Xylene

Similarly, reaction of **2** with $Ru_3(CO)_{12}$ gave the normal diruthenium complex **9** (13%) and a tetranuclear complex **10** (26%) (Scheme 2). The IR spectrum of **9** shows terminal and bridging carbonyl group absorptions at 1957 and 1774 cm^{-1}, similar to that of **7**. X-ray analysis confirms that **9** is a *trans* isomer (Figure 2). The IR spectrum of **10** shows only three terminal carbonyl group absorptions at 1962, 1918, and 1863 cm^{-1}. X-ray analysis shows that **10** is a C_i symmetrical tetranuclear complex with a flat butterfly metal framework and two indenyl ligands (Figure 3). The Ru–Ru distances (2.7266 to 2.8223 Å) are much shorter than those in $Ru_4(CO)_{13}(\mu\text{-}PPh_2)_2$ (2.9704–3.1776 Å).[13]

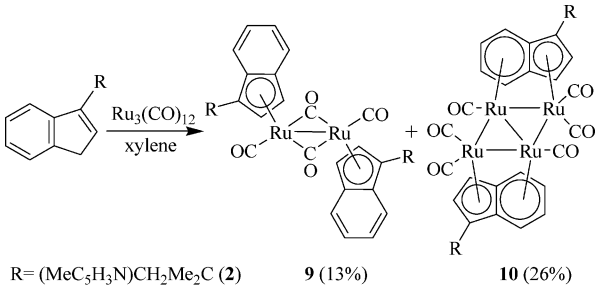

R= $(MeC_5H_3N)CH_2Me_2C$ (**2**)	**9** (13%)	**10** (26%)
*t*Bu (**3**)	**11** (22%)	**12** (3%)
$PhCH_2Me_2C$ (**4**)	**13** (9%)	**14** (8%)
$(C_{10}H_6N)CH_2Me_2C$ (**5**)	**15** (10%)	**16** (16%)

Scheme 2.

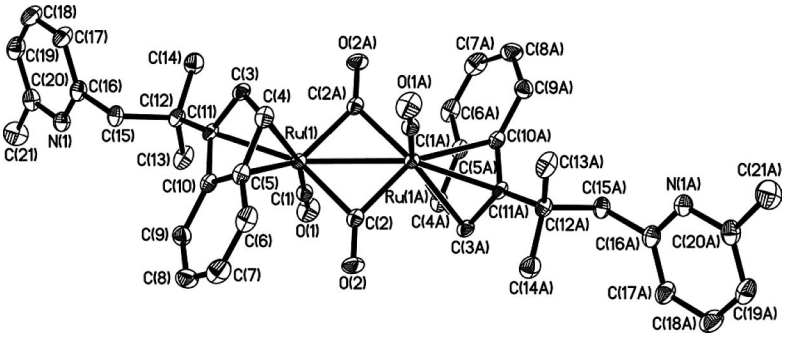

Figure 2. ORTEP diagram of **9**. Selected bond lengths [Å]: Ru(1)–Ru(1A) 2.7443(13).

The pyridyl groups only act as substituents and do not coordinate with the Ru atoms. The most noticeable structural feature of **10** is the bridging indenyl ligands, which coordinate with two ruthenium atoms in a *syn*-η^5:η^6-facial fashion. Bimetallic complexes with indenyl bridging facial ligands are scarce,[2,3] and only a few such complexes have ligands that bridge in a *syn*-facial fashion; therefore, complex **10** is a new example containing *syn*-η^5:η^6 bonding indenyl ligands.

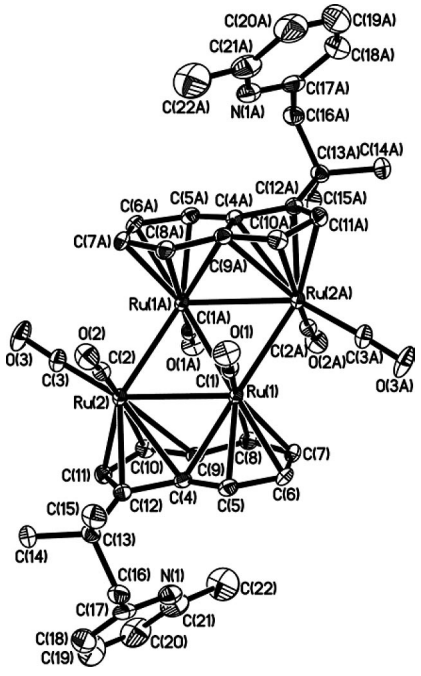

Figure 3. Molecular structure of **10**. Selected bond lengths [Å]: Ru(1)–Ru(1A) 2.7266(8), Ru(1)–Ru(2A) 2.7354(6), Ru(1)–Ru(2) 2.8223(6), Ru(1)–C(4) 2.419(5), Ru(1)–C(5) 2.224(5), Ru(1)–C(6) 2.234(5), Ru(1)–C(7) 2.296(5), Ru(1)–C(8) 2.367(5), Ru(1)–C(9) 2.464(5), Ru(2)–C(4) 2.499(4), Ru(2)–C(9) 2.573(4), Ru(2)–C(10) 2.319(5), Ru(2)–C(11) 2.210(5), Ru(2)–C(12) 2.282(5), C(4)–C(5) 1.431(6), C(4)–C(9) 1.450(6), C(5)–C(6) 1.421(7), C(6)–C(7) 1.398(7), C(7)–C(8) 1.407(7), C(8)–C(9) 1.415(6).

The only difference between **2** and **1** is the methyl substituent at the α-position of the pyridyl group. The α-C–H bond of the pyridyl ring in **1** can be activated by $Ru_3(CO)_{12}$,[14] which leads to the formation of **8**, in which the indenyl ligands are bound in a facial η^5:η^2:η^2 bonding mode.

Considering that the pyridyl groups of **10** do not coordinate with the Ru atoms, reactions of **3**–**5**, in which the pyridyl side chains were replaced by other bulky substituents [*t*Bu, $PhCH_2Me_2C$, and $(C_9H_6N)CH_2Me_2C$ (C_9H_6N = 2-quinolyl)], with $Ru_3(CO)_{12}$ were also done, and complexes with similar structures were obtained (Scheme 2). Single-crystal X-ray analysis showed that complex **14** also contains two *syn*-η^5:η^6 bonding indenyl groups, similar to that observed in **10** (Figure 4). This indicates that the steric effect of the bulky substituent in the 1-position of the indenyl ring

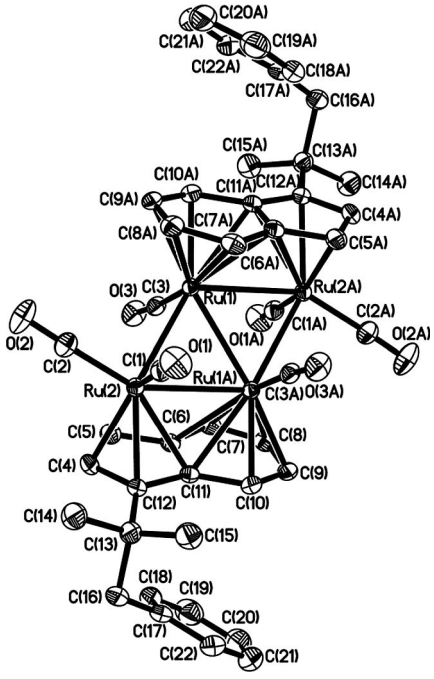

Figure 4. ORTEP diagram of **14**. Selected bond lengths [Å]: Ru(1)–Ru(1A) 2.7461(7), Ru(1)–Ru(2A) 2.8233(6), Ru(1)–Ru(2) 2.7287(5), Ru(1)–C(6A) 2.472(3), Ru(1)–C(7A) 2.370(4), Ru(1)–C(8A) 2.312(4), Ru(1)–C(9A) 2.245(3), Ru(1)–C(10A) 2.204(4), Ru(1)–C(11A) 2.408(3), Ru(2)–C(4) 2.205(4), Ru(2)–C(5) 2.314(4), Ru(2)–C(6) 2.562(3), Ru(2)–C(11) 2.499(3), Ru(2)–C(12) 2.269(4), C(6)–C(7) 1.408(5), C(6)–C(11) 1.455(5), C(7)–C(8) 1.398(5), C(8)–C(9) 1.394(5), C(9)–C(10) 1.412(5), C(10)–C(11) 1.436(5).

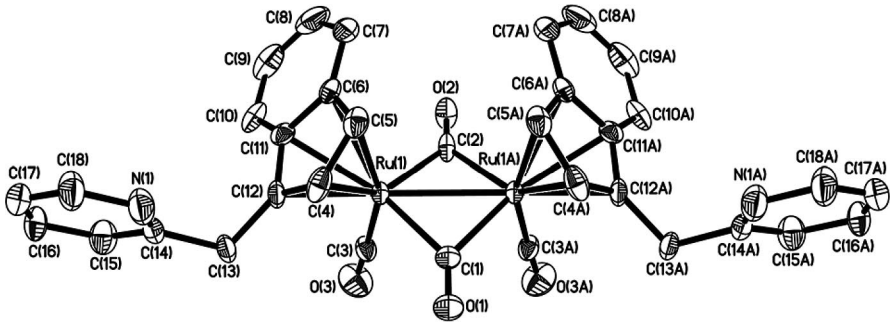

Figure 5. ORTEP diagram of **17**. Selected bond lengths [Å]: Ru(1)–Ru(1A) 2.7389(15).

may promote the formation of the *syn*-η^5:η^6 bonded indenyl tetranuclear ruthenium complexes. In contrast, reactions of 1-ferrocenyl, 1-$CH_2CH_2C_9H_7$, or 1,2,3-trimethyl-substituted indenes with $Ru_3(CO)_{12}$ only gave the normal η^5-indenyl diruthenium complexes.[15,1c] Reaction of 2-phenyl-substituted indene with $Ru_3(CO)_{12}$ also gave the η^5-indenyl diruthenium complex, in addition to a heptaruthenium cluster.[16]

Reaction of 6 with $Ru_3(CO)_{12}$ in Xylene

Thermal treatment of $Ru_3(CO)_{12}$ with **6**,[17] in which a short pyridyl side chain with smaller steric effects was introduced, gave the *cis* diruthenium complex **17** (3%) (Figure 5) and complex **18** (24%) (Scheme 3). Different with *trans* complexes **7** and **9**, *cis* complex **17** shows two terminal and two bridging carbonyl group absorptions at 1973 (s), 1936 (s), 1812 (m), and 1774 (s) cm^{-1} in its IR spectrum. The IR spectrum of **18** shows four terminal carbonyl group absorptions at 2000–1916 cm^{-1}. Single-crystal X-ray diffraction analysis shows that **18** is a diruthenium complex with two ligands (Figure 6). Each of the two N atoms coordinates with one Ru atom. One of the ligands is cyclometalated and coordinates with Ru(2) and Ru(1) in a η^1:η^2 mode. The bond lengths of C(20)–C(28) [1.464(4) Å] and C(27)–C(28) [1.481(4) Å] are significantly shorter than C(5)–C(6) [1.527(5) Å] and C(6)–C(7) [1.513(5) Å], which suggests that there are similarities between the η^1:η^2- and η^3-coordination modes. The other ligand coordinates with Ru(1) in a η^2 mode. The α-C of the pyridyl ring is bonded to the Ru(2) atom by C–H activation.

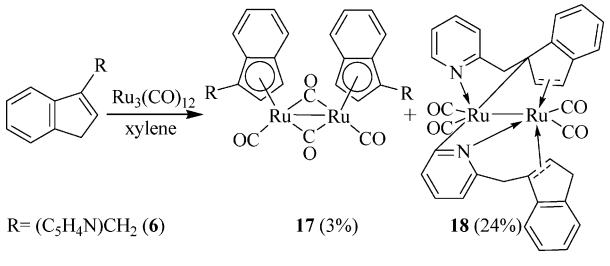

Scheme 3.

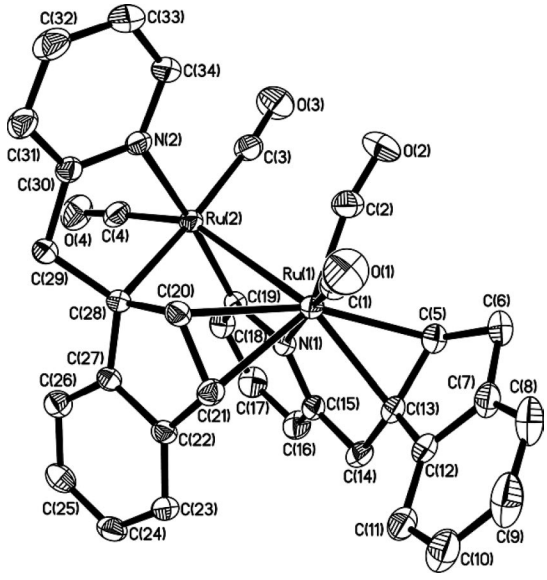

Figure 6. Molecular structure of **18**. Selected bond lengths [Å]: Ru(1)–Ru(2) 2.9448(5), Ru(1)–N(1) 2.088(2), Ru(1)–C(5) 2.228(3), Ru(1)–C(13) 2.256(3), Ru(1)–C(20) 2.371(3), Ru(1)–C(21) 2.323(3), Ru(2)–N(2) 2.188(2), Ru(2)–C(28) 2.211(3), Ru(2)–C(19) 2.044(3), C(5)–C(6) 1.527(5), C(5)–C(13) 1.421(4), C(20)–C(21) 1.414(4), C(20)–C(28) 1.464(4).

Reactions of 1, 2, and 5 with $Ru_3(CO)_{12}$ in Heptane

The high temperature of refluxing xylene might cause significant decomposition of $Ru_3(CO)_{12}$, so heptane was chosen as the solvent instead. When **1** or **2** was treated with $Ru_3(CO)_{12}$ in refluxing heptane, ionic clusters **19** (12%), **20** (34%), and complex **8** (5%) or ionic clusters **21** (13%) and **22** (25%) were obtained, respectively (Scheme 4). The total yield was merely a little higher than that in xylene, but different products were formed. When **5** was treated with $Ru_3(CO)_{12}$, only compound **23** (15%) was obtained. Compounds **19** and **21** show similar three carbonyl group absorptions at 2050–1954 cm^{-1} in their IR spectra and have similar ^1H NMR signals, which indicates that they have similar structures. X-ray diffraction analysis showed that **21** is an ionic cluster (Figure 7). The cation is a η^5-indenyl ruthenium complex with intramolecular coordination of the pyridyl group. The anion $[HRu_6(CO)_{18}]^-$ was discovered before.[14] Compounds **20**, **22**, and **23** have similar structures,

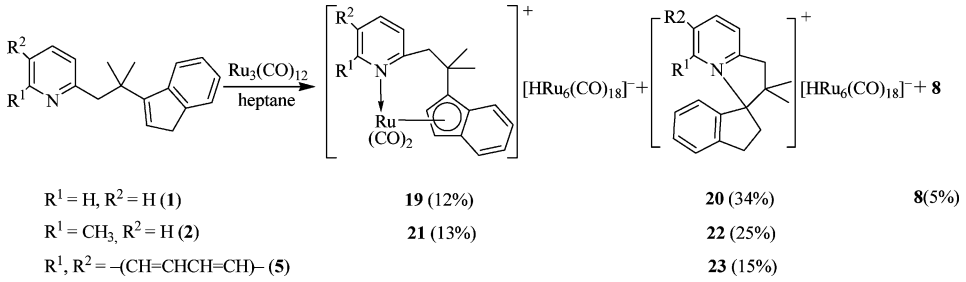

Scheme 4.

which was evidenced by their similar ^{1}H NMR spectra. The IR spectra of **20** and **23** showed two carbonyl group absorptions at 2012 and 1953 and at 2012 and 1954 cm^{-1}, respectively, whereas the IR spectrum of **22** showed four carbonyl group absorptions at 2054, 2018, 1998, and 1987 cm^{-1}. X-ray diffraction analysis showed that **22** is also an ionic cluster (Figure 8). The anion $[HRu_6(CO)_{18}]^-$ is the same as that in **21**, but the cation is a pyridinium ion with a spirocyclic structure. It seems that the formation of **20**, **22**, and **24** may involve cyclometalation, followed by reductive elimination (Scheme 5).[18]

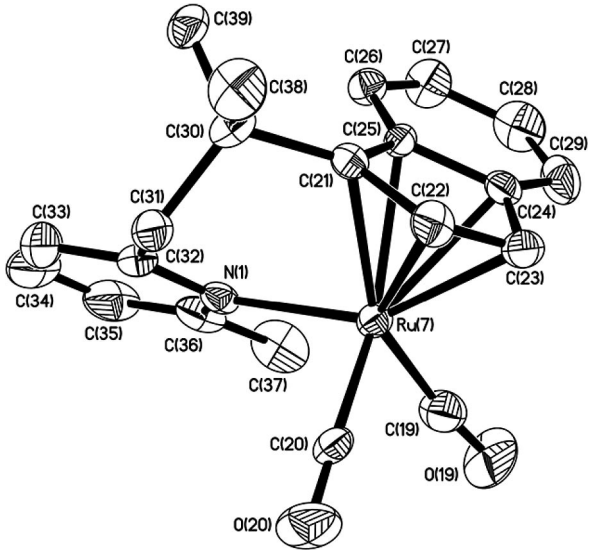

Figure 7. Structure of the cation of **21**.

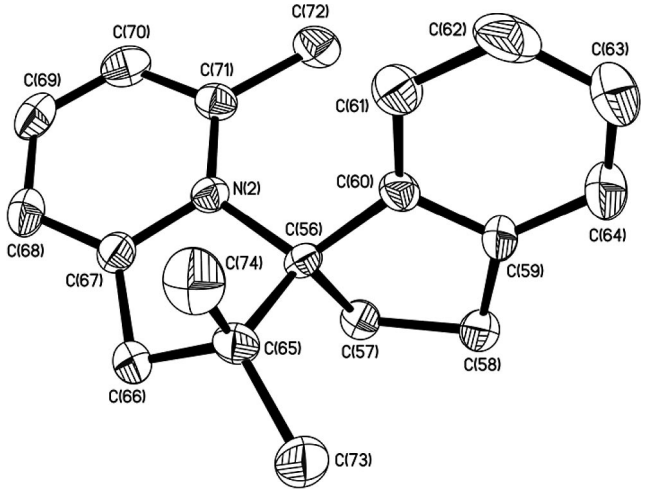

Figure 8. Structure of the cation of **22**.

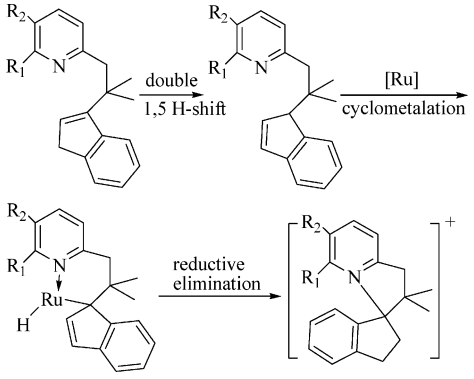

Scheme 5.

Reaction of 6 with $Ru_3(CO)_{12}$ in Heptane

When **6** was treated with $Ru_3(CO)_{12}$ in refluxing heptane, red ionic complex **24** was obtained, in addition to complex **18** (Scheme 6). The cation of **24** contains a Ru atom and two ligands with intramolecular coordination of the pyridyl group. One ligand coordinates with the Ru atom in a η^3 mode, whereas the other coordinates in a η^2 mode (Figure 9). Again, the anion is $[HRu_6(CO)_{18}]^-$.

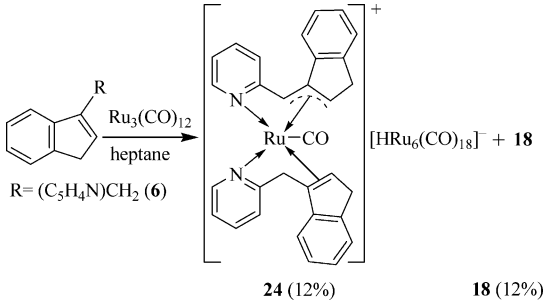

Scheme 6.

From the above results, we can see that the reaction solvents have significant effects on the formation of the products. Similar phenomenon was also reported in the reac-

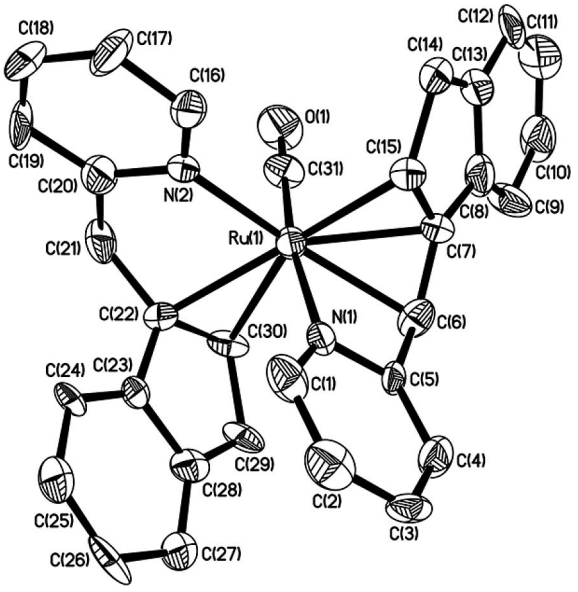

Figure 9. Structure of the cation of **24**.

tions of $Ru_3(CO)_{12}$ and $Os_3(CO)_{12}$.[5a,5b,5d,16,19] The solvent effect for this kind of thermal reaction is partly decided by the reaction temperature. When ligand precursor **2** was treated with $Ru_3(CO)_{12}$ in heptane at 140 °C, complex **10** was also isolated, in addition to **21** and **22**. However, no relationship between these complexes was found. So, the nature of the solvents plays the determined role in the formation of the products. The aromatic solvent, such as xylene, may act as an electron donor to coordinate with the metal and to promote or change the reactions.

^{1}H NMR Spectra Analysis

The ^{1}H NMR spectra of the normal η^5-coordinated indenyl diruthenium complexes **7**, **9**, **11**, **13**, **15**, and **17** are similar (Table 1). They all show three or four groups of peaks at 7.77–6.34 ppm for the C_6-ring protons of the indenyl ligand and two doublets or broad singlets at 5.61–4.44 ppm for the C_5-ring protons of the indenyl ligand. However, the chemical shifts of the benzo ring protons of **11** and **13** (7.77–6.65 ppm) are shifted downfield relative to those of the pyridyl or quinolyl side chain functionalized indenyl complexes **7**, **9**, **15**, and **17** (7.33–6.34 ppm), which is indicative of the effects of the N-heterocyclic side chains. The α,β-protons of the indenyl ring system and the CH_2 protons in the side chains were generally split into two characteristic doublets. It is easy to distinguish them by the large coupling constant (J^2) of the CH_2 protons. The ^{1}H NMR spectrum of **17** showed two groups of characteristic doublets for the five-membered protons of the indenyl unit, which indicates the existence of only one isomer. Dinuclear η^5-dienylruthenium complexes are usually obtained as mixtures of *cis* and *trans* isomers or as single *trans* isomers (such as **7** and **9**). There is only one example of a 2-phenylindenyl diruthenium complex $[(\eta^5\text{-}C_9H_6Ph)Ru(CO)(\mu\text{-}CO)]_2$ in which the *cis meso* isomer was obtained and characterized by X-ray diffraction analysis.[16] The reason why complex **17** exists as a single *cis meso* isomer is still not very clear. It seems that the existence of a picolyl (or phenyl) substituent on the indenyl ring may stabilize the *cis meso* isomer and promote its formation.

The most noticeable feature of the facial coordinated indenyl complexes **8**, **10**, **12**, **14**, and **16** in their ^{1}H NMR spectra is that nearly all resonances are shifted upfield rela-

Table 1. ^{1}H NMR data of complexes **7**, **9**, **11**, **13**, **15**, and **17** (in $CDCl_3$, ppm).

	Pyridyl H, quinolyl H, or C_6-ring H of indenyl	C_5-ring H of indenyl	Other H
7	8.42 (d, J = 4.9 Hz, 2 H)	5.19 (d, J = 3.0 Hz, 2 H)	3.26 (d, J = 13.0 Hz, 2 H, CH_2)
	7.66 (d, J = 8.7 Hz, 2 H)	4.48 (d, J = 3.0 Hz, 2 H)	3.13 (d, J = 13.0 Hz, 2 H, CH_2)
	7.39–7.28 (m, 4 H), 7.21–7.15 (m, 2 H)		1.84 (s, 6 H, CMe_2)
	7.04–6.98 (m, 4 H), 6.46 (d, J = 7.8 Hz, 2 H)		1.52 (s, 6 H, CMe_2)
9	7.58 (d, J = 8.7 Hz, 2 H), 7.34 (t, 2 H)	5.20 (br. s, 2 H)	3.28–2.98 (m, 4 H, CH_2)
	7.15 (m, 4 H), 7.00 (d, J = 8.4 Hz, 2 H)	4.49 (br. s, 2 H)	2.33 (s, 6 H, PyMe)
	6.86 (br. s, 2 H), 6.34 (d, J = 7.6 Hz, 2 H)		1.85 (s, 6 H, CMe_2)
			1.52 (s, 6 H, CMe_2)
11	7.77 (d, J = 8.5 Hz, 2 H), 7.33–7.19 (m, 4 H)	5.49 (d, J = 3.1 Hz, 2 H)	1.59 (s, 18 H, CMe_3)
	6.90 (d, J = 8.3 Hz, 2 H)	4.52 (d, J = 3.1 Hz, 2 H)	
13	7.71(d, J = 8.6 Hz, 2 H), 7.38 (t, 2 H)	5.07 (d, J = 3.1 Hz, 2 H)	3.11 (d, J = 13.1 Hz, 2 H, CH_2)
	7.24–7.02 (m, 10 H)	4.46 (d, J = 3.1 Hz, 2 H)	2.92 (d, J = 13.1 Hz, 2 H, CH_2)
	6.65 (d, J = 6.4 Hz, 4 H)		1.82 (s, 6 H, CMe_2)
			1.42 (s, 6 H, CMe_2)
15	7.87 (d, J = 8.4 Hz, 2 H)	5.13 (d, J = 3.0 Hz, 2 H)	3.46 (d, J = 12.4 Hz, 2 H, CH_2)
	7.74 (d, J = 8.4 Hz, 2 H)	4.44 (d, J = 3.0 Hz, 2 H)	3.30 (d, J = 12.4 Hz, 2 H, CH_2)
	7.69–7.60 (m, 6 H), 7.45 (t, 2 H)		1.91 (s, 6 H, CMe_2)
	7.33 (t, 2 H), 7.11 (t, 2 H)		1.56 (s, 6 H, CMe_2)
	7.01 (d, J = 8.4 Hz, 2 H)		
	6.56 (d, J = 8.4 Hz, 2 H)		
17	8.51 (d, J = 4.8 Hz, 2 H), 7.58 (t, 2 H)	5.61 (d, J = 3.0 Hz, 2 H)	4.32 (d, J = 15.3 Hz, 2 H, CH_2)
	7.40 (d, J = 7.8 Hz, 2 H), 7.33–7.22 (m, 4 H)	5.19 (d, J = 3.0 Hz, 2 H)	4.21 (d, J = 15.3 Hz, 2 H, CH_2)
	7.18 (d, J = 7.8 Hz, 2 H), 7.12 (t, 2 H)		
	7.05 (d, J = 7.8 Hz, 2 H)		

Table 2. ^{1}H NMR data of complexes **8**, **10**, **12**, **14**, **16**, and **18** (in $CDCl_3$, ppm).

	Pyridyl H, quinolyl H or C_6-ring H of indenyl	C_5-ring H of indenyl	Other H
8	7.47 (d, J = 7.5 Hz, 1 H), 7.07 (t, 1 H) 6.51 (d, J = 7.5 Hz, 1 H) 5.96 (d, J = 3.0 Hz, 1 H), 5.14 (m, 1 H) 3.52 (d, J = 3.0 Hz, 1 H), 3.35 (m, 1 H)	5.90 (d, J = 5.3 Hz, 1 H) 4.55 (d, J = 5.3 Hz, 1 H)	2.83(d, J = 14.2 Hz, 1 H, CH_2) 2.32 (d, J = 14.2 Hz, 1 H, CH_2) 1.60 (s, 3 H, CMe_2) 0.56 (s, 3 H, CMe_2)
10	7.37 (t, 2 H), 6.94 (d, J = 7.7 Hz, 2 H) 6.66 (d, J = 7.6 Hz, 2 H) 6.28 (d, J = 3.0 Hz, 2 H) 6.16 (t, 2 H), 5.54 (t, 2 H) 3.78 (d, J = 2.6 Hz, 2 H)	5.25 (d, J = 6.4 Hz, 2 H) 3.51 (d, J = 6.4 Hz, 2 H)	2.87 (m, 4 H, Py-CH_2) 1.20 (s, 6 H, CMe_2) 0.89 (s, 6 H, CMe_2) 2.41 (s, 6 H, Py-Me)
12	6.49 (d, J = 2.9 Hz, 2 H) 6.23 (t, 2 H), 5.77 (t, 2 H) 3.84 (d, J = 3.2 Hz, 2 H)	5.28 (d, J = 6.10 Hz, 2 H) 3.93 (d, J = 6.10 Hz, 2 H)	1.07 (s, 18 H, CMe_3)
14	7.21–7.15 (m, 6 H), 6.87–6.83(m, 4 H) 6.23 (d, J = 2.9 Hz, 2 H) 6.18 (t, 2 H), 5.60 (t, 2 H) 3.80 (d, J = 2.9 Hz, 2 H)	5.28 (d, J = 6.09 Hz, 2 H) 3.63 (d, J = 6.09 Hz, 2 H)	2.79 (d, J = 12.9 Hz, 2 H, CH_2) 2.67 (d, J = 12.9 Hz, 2 H, CH_2) 1.11 (s, 6 H, CMe_2) 0.86 (s, 6 H, CMe_2)
16	7.95–7.87 (m, 4 H), 7.76 (d, J = 8.6 Hz, 2 H) 7.68 (t, 2 H), 7.51 (t, 2 H) 6.96 (d, J = 8.4 Hz, 2 H) 6.28 (d, J = 2.9 Hz, 2 H) 6.04 (t, 2 H, Ar-H) 5.26–5.19 (m, 2 H) 3.75 (d, J = 2.3 Hz, 2 H)	5.26–5.19 (m, 2 H) 3.40 (d, J = 5.7 Hz, 2 H)	3.15 (d, J = 12.1 Hz, 2 H, CH_2) 3.04 (d, J = 12.1 Hz, 2 H, CH_2) 1.25 (s, 6 H, CMe_2) 0.95 (s, 6 H, CMe_2)
18	8.84 (d, J = 5.1 Hz, 1 H) 8.01 (d, J = 7.5 Hz, 1 H), 7.65 (m, 1 H) 7.44 (t, 1 H), 7.40–7.27 (m, 3 H) 7.40–7.27 (m, 1 H), 7.15 (m, 2 H) 6.76 (m, 1 H), 6.68 (m, 1 H) 6.29 (t, 1 H), 6.19 (d, J = 7.6 Hz, 1 H) 5.98 (d, J = 7.4 Hz, 1 H)	5.29 (d, J = 4.1 Hz, 1 H) 3.96 (m, 2 H) 3.88 (d, J = 6.0 Hz, 1 H) 3.60–3.51 (m, 1 H)	4.69 (d, J = 17.0 Hz, 1 H, CH_2) 3.81 (d, J = 17.0 Hz, 1 H, CH_2) 3.60–3.51 (m, 1 H, CH_2) 3.15 (d, J = 18.1 Hz, 1 H, CH_2)

tive to those of the corresponding η^5-coordinated indenyl complexes, especially for the benzo ring protons (from 7.77–6.34 to 6.49–3.35 ppm, see Table 2). This may be the result of the magnitude of back donation from the Ru atoms coordinated to the C_6 or C_5 ring. The η^5:η^2:η^2 coordination (5.96–3.35 ppm) shifts the resonances upfield relative to those observed for η^5:η^6-coordinated compounds (6.49–3.75 ppm).

The ^{1}H NMR spectrum of **18** shows 11 groups of peaks for the pyridyl and benzo ring protons at 8.84–5.98 ppm and 7 groups of peaks for the C_5-ring H and CH_2 protons at 5.29–3.15 ppm, which is indicative of the unsymmetrical structure. It is consistent with the X-ray diffraction analysis results. Similar to that mentioned above, most of the chemical shifts of the corresponding protons in **18** are also shifted upfield relative to those in **17**.

The ^{1}H NMR spectra of the anions of compounds **19**–**24** are almost identical and show a singlet at about 16.4 ppm (Table 3), which is consistent with the values reported earlier.[20] One of the four H atoms [H(57A)] of the C_5 ring of the indenyl group in **22** (2.21–2.11 ppm) is shifted upfield relative to the other three H atoms (3.24–3.02 ppm); this is possibly due to the deshielding effect of the surrounding groups (Figure 8). This phenomenon also appears in compounds **20** and **23**.

Conclusion

A series of metal complexes with different bonding modes of the indenyl ligand was prepared by reaction of pyridyl side chain functionalized indenes with $Ru_3(CO)_{12}$ in refluxing xylene. The results clearly show the effects of the functionalized side chain on the reaction. The existence of a bulky substituent on the indenyl ring may promote the formation of the *syn*-η^5:η^6-bonded indenyl clusters. The solvent also has a significant effect on the reaction, and a series of ionic clusters were obtained when heptane was used instead of xylene.

Experimental Section

General Considerations: Schlenk and vacuum line techniques were employed for all manipulations of air- and moisture-sensitive compounds. All solvents were distilled from appropriate drying agents under an atmosphere of argon before use. ^{1}H NMR spectra were recorded with a Bruker AV300 or VARIAN AS-400, and IR spectra were recorded as KBr disks with a Nicolet 5DX FTIR spectrometer. Mass spectra were obtained from a VG ZAB-HS. Elemental analyses were performed with a Perkin–Elmer 240C analyzer. Ligand precursors **1**,[9] **3**,[21] and **6**[17] were synthesized according to literature procedures.

Ligand Precursor 2: The ligand precursor **2** was prepared following the procedure as described for ligand precursor **1**.[9] A solution of 6,6′-dimethylbenzofulvene (10.2 g, 65.4 mmol) in Et_2O (50 mL) was added to a solution prepared from 2,6-dimethylpyridine (7.00 g, 65.4 mmol) in *n*-hexane (100 mL) and *n*BuLi (41.5 mL, 50.7 mmol). The mixture was stirred overnight at room temperature and hydrolyzed with water. After separation and drying, the solvents were removed under reduced pressure. The resulting oil was distilled, and a yellow fraction at 140–143 °C/0.3 Torr was collected (11.9 g, 69%). ^{1}H NMR (300 MHz, $CDCl_3$): δ = 7.78 (d, J =

Table 3. ^{1}H NMR data of complexes **19**–**24** (in $CDCl_3$, ppm).

	$[HRu_6(CO)_{18}]^-$	Pyridyl H, quinolyl H or C_6-ring H of indenyl	C_5-ring H of indenyl	Other H
19	16.46 (s, 1 H)	8.14 (d, J = 5.4 Hz, 1 H) 8.06 (t, 1 H) 7.71 (d, J = 7.4 Hz, 1 H) 7.56 (d, J = 4.1 Hz, 2 H) 7.39–7.29 (m, 2 H) 7.18 (d, J = 8.7 Hz, 1 H)	6.13 (d, J = 2.6 Hz, 1 H) 5.45 (d, J = 2.6 Hz, 1 H)	3.49 (d, J = 14.4 Hz, 1 H, Py-CH_2) 3.08 (d, J = 14.4 Hz, 1 H, Py-CH_2) 1.63 (d, J = 3.5 Hz, 6 H, Me)
20	16.41 (s, 1 H)	8.51 (t, 1 H) 8.30 (d, J = 5.8 Hz, 1 H) 8.04 (d, J = 7.2 Hz, 1 H) 7.92 (t, 1 H) 7.59–7.48 (m, 2 H) 7.40 (m, 1 H) 7.02 (d, J = 7.6 Hz, 1 H)	3.24–3.02 (m, 3 H) 2.21–2.11 (m, 1 H)	3.62 (d, J = 17.7 Hz, 1 H, Py-CH_2) 3.46 (d, J = 17.7 Hz, 1 H, Py-CH_2) 1.34 (s, 3 H, Me), 1.09 (s, 3 H, Me)
21	16.47 (s, 1 H)	7.90 (t, 1 H) 7.76 (d, J = 8.4 Hz, 1 H) 7.56 (m, 2 H) 7.42 (m, 2 H) 6.87 (d, J = 8.9 Hz, 1 H)	6.41 (d, J = 2.8 Hz, 1 H) 5.53 (d, J = 2.8 Hz, 1 H)	3.44 (d, J = 14.3 Hz, 1 H, Py-CH_2) 3.14 (d, J = 14.3 Hz, 1 H, Py-CH_2) 1.97 (s, 3 H, Me), 1.77 (s, 3 H, Me) 1.53 (s, 3 H, Me)
22	16.40 (s, 1 H)	8.30 (t, 1 H) 7.81 (d, J = 7.5 Hz, 1 H) 7.61 (d, J = 7.5 Hz, 1 H), 7.50 (m, 2 H) 7.36 (t, 1 H) 7.11 (d, J = 8.3 Hz, 1 H)	3.24–3.03 (m, 3 H) 2.39–2.30 (m, 1 H)	3.57 (d, J = 17.3 Hz, 1 H, Py-CH_2), 3.35 (d, J = 17.3 Hz, 1 H, Py-CH_2) 2.23 (s, 3 H, Me), 1.26 (s, 3 H, Me) 1.09 (s, 3 H, Me)
23	16.38 (s, 1 H)	8.91 (d, J = 8.3 Hz, 1 H) 8.26 (d, J = 8.2 Hz, 1 H) 7.96 (d, J = 8.3 Hz, 1 H) 7.87 (t, 1 H), 7.74 (t, 1 H) 7.61–7.52 (m, 2 H) 7.31–7.22 (m, 2 H) 6.90 (d, J = 7.7 Hz, 1 H)	3.29 (t, 2 H) 3.12–3.02 (m, 1 H) 2.68–2.56 (m, 1 H)	3.76 (d, J = 17.8 Hz, 1 H, Quin-CH_2) 3.58 (d, J = 17.8 Hz, 1 H, Quin-CH_2), 1.35 (s, 3 H, Me), 1.12 (s, 3 H, Me)
24	16.45 (s, 1 H)	9.33 (d, J = 5.3 Hz, 1 H) 8.14 (m, 1 H) 7.87 (d, J = 7.9 Hz, 1 H) 7.74–7.64 (m, 2 H) 7.55–7.44 (m, 2 H) 7.11 (t, 2 H) 6.98–6.90 (m, 2 H) 6.80 (d, J = 7.5 Hz, 1 H) 6.69–6.61 (m, 2 H), 6.54–6.48 (m, 1 H) 6.32 (d, J = 5.1 Hz, 1 H)	5.23 (s, 1 H), 4.58 (d, J = 16.5 Hz, 1 H) 4.38 (d, J = 4.0 Hz, 1 H), 3.93–3.67 (m, 4 H) 3.38 (d, J = 21.7 Hz, 1 H), 3.20 (d, J = 21.7 Hz, 1 H) (C_5-ring H, Py-CH_2 and Py-CH)	

7.7 Hz, 1 H, Py-H), 7.49 (d, J = 7.3 Hz, 1 H, Py-H), 7.33 (t, J = 7.3 Hz, 1 H, Py-H), 7.22 (dd, J = 7.7 Hz, J = 6.5 Hz, 2 H, Ar-H), 6.89 (d, J = 7.6 Hz, 1 H, Ar-H), 6.44 (d, J = 7.7 Hz, 1 H, Ar-H), 6.06 (t, J = 2.1 Hz, 1 H, C_5-ring H), 3.26 (br. s, 4 H, C_5-ring H and Py-CH_2), 2.51 (s, 3 H, Py-Me), 1.37 (s, 6 H, CMe_2) ppm. ^{13}C NMR (75 MHz, $CDCl_3$): δ = 158.9, 157.0, 151.6, 145.7, 144.0, 135.5, 128.3, 125.8, 124.1, 124.0, 122.2, 121.1, 120.4, 48.5, 37.6, 37.2, 27.4, 24.6 ppm. MS (ESI/CH_2Cl_2): m/z = 264 $[M + H]^+$. $C_{19}H_{21}N$ (263.17): calcd. C 86.65, H 8.04, N 5.32; found C 86.50, H 8.02, N 5.41.

Ligand Precursor 4: A solution of 6,6′-dimethylbenzofulvene (15.6 g, 100 mmol) in THF (60 mL) was added to a solution of $PhCH_2MgCl$ in THF, which was prepared from $PhCH_2Cl$ (12.7 g, 100 mmol) in THF (100 mL) and Mg (2.4 g, 100 mmol). The mixture was heated at reflux for 12 h and then hydrolyzed with water. After separation and drying, the solvents were removed under reduced pressure. The resulting oil was distilled, and a yellow fraction at 130–133 °C/0.05 Torr was collected (5.33 g, 22%). ^{1}H NMR (300 MHz, $CDCl_3$): δ = 7.78 (d, J = 7.6 Hz, 1 H, Ar-H), 7.49 (d, J = 7.3 Hz, 1 H, Ar-H), 7.36–7.09 (m, 5 H, Ar-H), 6.93–6.87 (m, 2 H, Ar-H), 6.01 (t, J = 2.1 Hz, 1 H, C_5-ring H), 3.25 (s, 2 H), 3.07 (s, 2 H, C_5-ring H and Ar-CH_2), 1.33 (s, 6 H, CMe_2) ppm. ^{13}C NMR (75 MHz, $CDCl_3$): δ = 151.3, 145.8, 144.1, 139.1, 130.4, 128.5, 127.5, 125.8, 125.7, 124.2, 124.1, 122.3, 46.6, 37.6, 37.3, 27.5 ppm. MS (EI): m/z = 248 $[M]^+$. $C_{19}H_{20}$ (248.16): calcd. C 91.88, H 8.12; found C 92.01, H 7.95.

Ligand Precursor 5: By using a similar procedure to that described for **2**, ligand precursor **5** was prepared from 2-methylquinoline, *n*BuLi, and 6,6′-dimethylbenzofulvene in 98% yield as a yellow solid. M.p. 94–95 °C. ^{1}H NMR (400 MHz, $CDCl_3$): δ = 8.09 (d, J = 8.4 Hz, 1 H), 7.87 (d, J = 7.7 Hz, 1 H), 7.80 (d, J = 8.5 Hz, 1 H), 7.71 (d, J = 8.2 Hz, 1 H), 7.67 (d, J = 8.1 Hz, 1 H), 7.53 (d, J = 7.4 Hz, 1 H), 7.47 (t, J = 7.5 Hz, 1 H), 7.38 (t, J = 7.5 Hz, 1 H), 7.26 (t, J = 7.4 Hz, 1 H), 6.74 (d, J = 8.5 Hz, 1 H, Quin and Ar-

H), 6.04 (s, 1 H, C_5-ring H), 3.50 (s, 2 H), 3.27 (s, 2 H, C_5-ring H and Quin-CH_2), 1.45 (s, 6 H, CMe_2) ppm. ^{13}C NMR (100 MHz, $CDCl_3$): δ = 160.3, 151.2, 147.7, 145.8, 143.9, 135.0, 129.2, 129.2, 128.6, 127.4, 126.7, 125.9, 125.7, 124.3, 122.7, 122.2, 49.3, 37.9, 37.3, 27.7 ppm. MS (ESI/CH_2Cl_2): m/z = 300 $[M + H]^+$. $C_{22}H_{21}N$ (299.17): calcd. C 88.25, H 7.07, N 4.68; found C 88.21, H 7.10, N 4.65.

Reaction of 1 with $Ru_3(CO)_{12}$ in Xylene: A solution of $Ru_3(CO)_{12}$ (0.300 g, 0.469 mmol) and ligand precursor **1** (0.351 g, 1.41 mmol) in xylene (30 mL) was heated at reflux for 5 h. The solvent was removed under reduced pressure, and the residue was placed in an Al_2O_3 column. Elution with CH_2Cl_2/petroleum ether developed two bands. The first band gave 0.090 g (29%) of **8** as red crystals, and the second band yielded 0.080 g (14%) of **7** as orange crystals. Data for **7**: M.p. 210–211 °C. IR (KBr, ν_{CO}): $\tilde{\nu}$ = 1957 (s), 1770 (s) cm^{-1}. $C_{40}H_{36}N_2O_4Ru_2$ (812.08): calcd. C 59.25, H 4.47, N 3.45; found C 59.50, H 4.53, N 3.40. Data for **8**: M.p. 135 °C (dec.). IR (KBr, ν_{CO}): $\tilde{\nu}$ = 2034 (s), 1997 (s), 1977 (s), 1960 (s), 1952 (s), 1938 (s), 1902 (s), 1851 (s) cm^{-1}. $C_{26}H_{17}NO_8Ru_4$ (878.71): calcd. C 35.66, H 1.96, N 1.60; found C 35.38, H 2.01, N 1.62.

Reaction of 2 with $Ru_3(CO)_{12}$ in Xylene: By using a similar procedure to that described above, reaction of ligand precursor **2** with $Ru_3(CO)_{12}$ gave red product **10** and orange product **9** in 26 and 13% yield, respectively. Data for **9**: M.p. 215–216 °C. IR (KBr, ν_{CO}): $\tilde{\nu}$ = 1957 (s), 1774 (s) cm^{-1}. $C_{42}H_{40}N_2O_4Ru_2$ (840.11): calcd. C 59.99, H 4.80, N 3.33; found C 59.92, H 4.85, N 3.47. Data for **10**: M.p. 170–171 °C. IR (KBr, ν_{CO}): $\tilde{\nu}$ = 1962 (s), 1918 (s), 1863 (s) cm^{-1}. $C_{44}H_{40}N_2O_6Ru_4$ (1099.91): calcd. C 8.00, H 3.67, N 2.55; found C 48.11, H 3.62, N 2.48.

Reaction of 3 with $Ru_3(CO)_{12}$ in Xylene: By using a similar procedure to that described above, reaction of ligand precursor **3** with $Ru_3(CO)_{12}$ gave red product **12** and orange product **11** in 3 and 22% yield, respectively. Data for **11**: M.p. 73–74 °C. IR (KBr, ν_{CO}): $\tilde{\nu}$ = 1954 (s), 1778 (s) cm^{-1}. $C_{30}H_{30}O_4Ru_2$ (658.02): calcd. C 54.87, H 4.60; found C 55.10, H 4.85. Data for **12**: M.p. 141–142 °C. IR (KBr, ν_{CO}): $\tilde{\nu}$ = 1974 (s), 1931 (s), 1878 (m) cm^{-1}. $C_{32}H_{30}O_6Ru_4$ (917.82): calcd. C 42.01, H 3.31; found C 41.91, H 3.38.

Reaction of 4 with $Ru_3(CO)_{12}$ in Xylene: By using a similar procedure to that described above, reaction of ligand precursor **4** with $Ru_3(CO)_{12}$ gave red product **14** and orange product **13** in 8 and 9% yield, respectively. Data for **13**: M.p. 210 °C (dec.). IR (KBr, ν_{CO}): $\tilde{\nu}$ = 1954 (s), 1781(s) cm^{-1}. $C_{42}H_{38}O_4Ru_2$ (810.09): calcd. C 62.36, H 4.74; found C 62.08, H 4.65. Data for **14**: M.p. 210–212 °C (dec.). IR (KBr, ν_{CO}): $\tilde{\nu}$ = 1968 (s), 1917 (s), 1880 (m) cm^{-1}. $C_{44}H_{38}O_6Ru_4$ (1069.88): calcd. C 49.53, H 3.59; found C 49.49, H 3.46.

Reaction of 5 with $Ru_3(CO)_{12}$ in Xylene: By using a similar procedure to that described above, reaction of ligand precursor **5** with $Ru_3(CO)_{12}$ gave red product **16** and orange product **15** in 16 and 10% yield, respectively. Data for **15**: M.p. 215–216 °C. IR (KBr, ν_{CO}): $\tilde{\nu}$ = 1946 (s), 1782 (s) cm^{-1}. $C_{48}H_{40}N_2O_4Ru_2$ (912.11): calcd. C 63.28, H 4.43, N 3.08; found C 63.48, H 4.64, N 3.19. Data for **16**: M.p. 140–141 °C. IR (KBr, ν_{CO}): $\tilde{\nu}$ = 1965 (s), 1923 (s), 1871 (m) cm^{-1}. $C_{50}H_{40}N_2O_6Ru_4$ (1171.91): calcd. C 51.37, H 3.45, N 2.40; found C 51.42, H 3.63, N 2.48.

Reaction of 6 with $Ru_3(CO)_{12}$ in Xylene: By using a similar procedure to that described above, reaction of ligand precursor **6** with $Ru_3(CO)_{12}$ gave yellow product **18** and orange product **17** in 24 and 3% yield, respectively. Data for **17**: M.p. 130–131 °C. IR (KBr, ν_{CO}): $\tilde{\nu}$ = 1973 (s), 1936 (s), 1812 (m), 1774 (s) cm^{-1}. $C_{34}H_{24}N_2O_4Ru_2$ (727.98): calcd. C 56.19, H 3.33, N 3.85; found C 59.10, H 3.15, N 3.72. Data for **18**: M.p. 180 °C (dec.). IR (KBr, ν_{CO}): $\tilde{\nu}$ = 2000 (s), 1977 (s), 1924 (s), 1916 (s) cm^{-1}. $C_{34}H_{24}N_2O_4Ru_2$ (727.98): calcd. C 56.19, H 3.33, N 3.85; found C 56.15, H 3.56, N 4.08.

Reaction of 1 with $Ru_3(CO)_{12}$ in Heptane: A solution of $Ru_3(CO)_{12}$ (0.300 g, 0.469 mmol) and **1** (0.117 g, 0.469 mmol) in heptane (30 mL) was heated at reflux for 15 h. The solvent was removed under reduced pressure, and the residue was placed in an Al_2O_3 column. Elution with CH_2Cl_2/petroleum ether gave products **8** (0.020 g), **19** (0.037 g), and **20** (0.11 g) in 5, 12, and 34% yield,

Table 4. Crystal data and summary of X-ray data collection for **8**–**10**, **14**, and **17**.

	8·CH_2Cl_2	**9**	**10**·CH_2Cl_2	**14**	**17**
Formula	$C_{53}H_{36}Cl_2N_2O_{16}Ru_8$	$C_{42}H_{40}N_2O_4Ru_2$	$C_{23}H_{22}Cl_2NO_3Ru_2$	$C_{22}H_{19}O_3Ru_2$	$C_{34}H_{24}N_2O_4Ru_2$
Fw	1836.30	838.90	633.46	533.51	726.69
T [K]	294(2)	293(2)	293(2)	294(2)	294(2)
Crystal system	triclinic	triclinic	triclinic	monoclinic	orthorhombic
Space group	$P\bar{1}$	$P\bar{1}$	$P\bar{1}$	$P2_1/c$	$Pnma$
a [Å]	10.363(6)	6.579(3)	8.7574(15)	11.396(2)	15.803(4)
b [Å]	15.225(8)	8.754(4)	9.6907(17)	8.4280(16)	27.645(7)
c [Å]	18.276(11)	16.552(7)	14.913(3)	19.785(4)	6.5968(17)
α [°]	81.680(9)	95.354(6)	79.430(3)	90	90
β [°]	81.218(9)	99.032(6)	86.417(3)	90.058(3)	90
γ [°]	74.191(9)	110.662(6)	70.619(2)	90	90
V [Å^3]	2726(3)	869.5(6)	1173.7(4)	1900.4(6)	2881.9(12)
Z	2	1	2	4	4
$D_{calcd.}$ [g cm^{-3}]	2.237	1.602	1.792	1.865	1.675
μ [mm^{-1}]	2.324	0.915	1.539	1.609	1.090
F(000)	1764	426	626	1052	1448
Crystal size [mm]	0.38 × 0.34 × 0.30	0.30 × 0.12 × 0.12	0.14 × 0.10 × 0.06	0.40 × 0.20 × 0.12	0.22 × 0.20 × 0.12
θ range [°]	1.13–25.01	1.26–26.14	1.39–25.01	1.79–26.29	1.47–25.01
No. of reflns collected	14344	4881	6151	10329	12992
No. of indep. reflns/R_{int}	9562/0.0170	3403/0.0359	4134/0.0233	3857/0.0326	2549/0.0694
No. of parameters	734	229	283	246	196
Goodness-of-fit on F^2	1.077	1.055	1.107	1.102	1.183
R_1, wR_2 [$I > 2\sigma(I)$]	0.0267, 0.0605	0.0503, 0.1294	0.0306, 0.0743	0.0285, 0.0694	0.0678, 0.1250
R_1, wR_2 (all data)	0.0379, 0.0667	0.0587, 0.1414	0.0449, 0.0931	0.0452, 0.0757	0.1114, 0.1549

Table 5. Crystal data and summary of X-ray data collection for **18**, **21**, **22**, and **24**.

	18	**21**·CH_2Cl_2	**22**·CH_2Cl_2	**24**
Formula	$C_{34}H_{24}N_2O_4Ru_2$	$C_{39.50}H_{22}ClNO_{20}Ru_7$	$C_{37.50}H_{24}ClNO_{18}Ru_6$	$C_{49}H_{26}N_2O_{19}Ru_7$
Fw	726.69	1573.52	1418.45	1654.24
T [K]	294(2)	293(2)	294(2)	293(2)
Crystal system	monoclinic	monoclinic	monoclinic	triclinic
Apace group	$C2/c$	$P2_1/c$	$P2_1/n$	$P\bar{1}$
a [Å]	15.2648(18)	10.0159(10)	24.314(3)	15.363(3)
b [Å]	15.9920(19)	14.3530(14)	14.1785(17)	19.088(3)
c [Å]	24.900(3)	33.460(3)	27.035(3)	20.472(4)
α [°]	90	90	90	95.687(4)
β [°]	106.971(2)	92.466(2)	104.731(2)	100.448(4)
γ [°]	90	90	90	113.147(3)
V [Å^3]	5813.9(12)	4805.7(8)	9013.4(18)	5331.4(17)
Z	8	4	8	4
$D_{calcd.}$ [g cm^{-3}]	1.660	2.175	2.091	2.060
μ [mm^{-1}]	1.081	2.272	2.092	2.004
$F(000)$	2896	3004	5448	3172
Crystal size [mm]	$0.28 \times 0.22 \times 0.20$	$0.18 \times 0.12 \times 0.10$	$0.32 \times 0.24 \times 0.20$	$0.22 \times 0.14 \times 0.04$
θ range [°]	1.71–26.38	1.226–26.38	1.01–26.40	1.03–25.02
No. of reflns collected	16187	26818	50442	27306
No. of indep. reflns/R_{int}	5940/0.0286	9786/0.0648	18356/0.0546	18707/0.0884
No. of parameters	379	634	1148	1522
Goodness-of-fit on F^2	1.079	0.988	1.011	1.019
R_1, wR_2 [$I > 2\sigma(I)$]	0.0286, 0.0623	0.0449, 0.0844	0.0535, 0.1225	0.0790, 0.1600
R_1, wR_2 (all data)	0.0468, 0.0704	0.1062, 0.1043	0.1065, 0.1491	0.2398, 0.2404

respectively. Data for **19**: M.p. 137 °C (dec.). IR (KBr, ν_{CO}): $\tilde{\nu}$ = 2050 (s), 2010 (s), 1954 (s) cm^{-1}. $C_{38}H_{19}NO_{20}Ru_7$ (1522.38): calcd. C 30.09, H 1.26, N 0.92; found C 30.57, H 1.74, N 1.11. Data for **20**: M.p. 140–141 °C. IR (KBr, ν_{CO}): $\tilde{\nu}$ = 2012 (s), 1953 (s) cm^{-1}. $C_{36}H_{21}NO_{18}Ru_6$ (1366.50): calcd. C 31.75, H 1.55, N 1.03; found C 32.01, H 1.72, N 1.37.

Reaction of 2 with $Ru_3(CO)_{12}$ in Heptane: By using a similar procedure to that described above, reaction of **2** (0.370 g, 1.41 mmol) with $Ru_3(CO)_{12}$ (0.300 g, 0.469 mmol) gave red products **21** (0.040 g) and **22** (0.080 g) in 13 and 25% yield, respectively. Data for **21**: M.p. 125 °C (dec.). IR (KBr, ν_{CO}): $\tilde{\nu}$ = 2056 (w), 2022 (s), 1957 (w) cm^{-1}. $C_{39}H_{21}NO_{20}Ru_7$ (1536.40): calcd. C 30.59, H 1.38, N 0.91; found C 30.40, H 1.45, N 1.00. Data for **22**: M.p. 118 °C (dec.). IR (KBr, ν_{CO}): $\tilde{\nu}$ = 2054 (s), 2018 (s), 1998 (s), 1987 (m) cm^{-1}. $C_{37}H_{23}NO_{18}Ru_6$ (1380.52): calcd. C 32.30, H 1.68, N 1.02; found C 32.65, H 1.85, N 1.16.

Reaction of 5 with $Ru_3(CO)_{12}$ in Heptane: By using a similar procedure to that described above, reaction of **5** (0.421 g, 1.41 mmol) with $Ru_3(CO)_{12}$ (0.300 g, 0.469 mmol) gave red product **23** (0.050 g) in 15% yield. Data for **23**: M.p. 135 °C (dec.). IR (KBr, ν_{CO}): $\tilde{\nu}$ = 2012 (s), 1954 (s) cm^{-1}. $C_{40}H_{23}NO_{18}Ru_6$ (1416.52): calcd. C 34.02, H 1.64, N 0.99; found C 33.78, H 1.92, N 1.03.

Reaction of 6 with $Ru_3(CO)_{12}$ in Heptane: By using a similar procedure to that described above, reaction of **6** (0.292 g, 1.41 mmol) with $Ru_3(CO)_{12}$ (0.300 g, 0.469 mmol) gave yellow product **18** (0.060 g) and red product **24** (0.040 g) both in 12% yield. Data for **24**: M.p. 130 °C (dec.). IR (KBr, ν_{CO}): $\tilde{\nu}$ = 2014 (s), 1952 (s) cm^{-1}. $C_{49}H_{26}N_2O_{19}Ru_7$ (1659.44): calcd. C 35.58, H 1.58, N 1.69; found C 35.80, H 1.85, N 2.06.

Crystallographic Studies: Single crystals of complexes **8**, **9**, **10**, **14**, **17**, **18**, **21**, **22**, and **24** suitable for X-ray diffraction were obtained from hexane/CH_2Cl_2 solutions. Data collection was performed with a BRUKER SMART 1000 by using graphite-monochromated Mo-K_α radiation (ω-2θ scans, λ = 0.71073 Å). Semiempirical absorption corrections were applied for all complexes. The structures were solved by direct methods and refined by full-matrix least-squares. All calculations were performed by using the SHELXL-97 program system. The crystal data and summary of X-ray data collection are presented in Tables 4 and 5. CCDC-636913 (for **8**), -636914 (for **9**), -636915 (for **10**), -655292 (for **14**), -636916 (for **17**), -636917 (for **18**), -666253 (for **21**), -666254 (for **22**), and -666255 (for **24**) contain the supplementary crystallographic data for this paper. These data can be obtained free of charge from The Cambridge Crystallographic Data Centre via www.ccdc.cam.ac.uk/data_request/cif.

Acknowledgments

We are grateful to the National Natural Science Foundation of China (20672058, 20574036, 20421202), the Program for New Century Excellent Talents in University (NCET-04–0229), and the Research Fund for the Doctoral Program of Higher Education of China (20070055020) for financial support.

[1] For recent reviews on the chemistry of indenyl metal complexes, see: a) A. Togni, R. L. Halterman (Eds.), *Metallocenes: Synthesis Reactivity, Applications*, Wiley-VCH, Weinheim, **1998**; b) C. Bonifaci, A. Ceccon, A. Gambaro, F. Manoli, L. Mantovani, P. Ganis, S. Santi, A. Venzo, *J. Organomet. Chem.* **1998**, *577*, 97–109; c) V. Cadierno, J. Diez, M. P. Gamasa, J. Gimeno, E. Lastra, *Coord. Chem. Rev.* **1999**, *193–195*, 147–205; d) M. J. Calhorda, L. F. Veiros, *Coord. Chem. Rev.* **1999**, *185–186*, 37–51; e) L. Resconi, L. Cavallo, A. Fait, F. Piemontesi, *Chem. Rev.* **2000**, *100*, 1253–1346; f) M. Stradiotto, M. J. Mcglinchey, *Coord. Chem. Rev.* **2001**, *219–221*, 311–378; g) M. J. Calhorda, V. Félix, L. F. Veiros, *Coord. Chem. Rev.* **2002**, *230*, 49–64; h) D. Zargarian, *Coord. Chem. Rev.* **2002**, *233–234*, 157–176; i) A. Ceccon, S. Santi, L. Orian, A. Bisello, *Coord. Chem. Rev.* **2004**, *248*, 683–724.

[2] M. E. Rerek, L.-N. Ji, F. Basolo, *J. Chem. Soc., Chem. Commun.* **1983**, 1208–1209.

[3] For *anti*-μ-indenyl bimetallic complexes, see: a) M. L. H. Green, N. D. Lowe, D. O'Hare, *J. Chem. Soc., Chem. Commun.* **1986**, 1547–1548; b) A. Ceccon, A. Gambaro, S. Santi, G. Valle, A. Venzo, *J. Chem. Soc., Chem. Commun.* **1989**, 51–53;

c) A. Ceccon, A. Gambaro, S. Santi, A. Venzo, *J. Mol. Catal.* **1991**, *69*, L1–L6; d) A. R. Kudinov, P. V. Petrovskii, Y. T. Struchkov, A. I. Yanovskii, M. I. Rybinskaya, *J. Organomet. Chem.* **1991**, *421*, 91–115; e) A. Ceccon, C. J. Elsevier, J. M. Ernsting, A. Gambaro, S. Santi, A. Venzo, *Inorg. Chim. Acta* **1993**, *204*, 15–26; f) C. Bonifaci, A. Ceccon, A. Gambaro, P. Ganis, L. Mantovani, S. Santi, A. Venzo, *J. Organomet. Chem.* **1994**, *475*, 267–276; g) C. Bonifaci, A. Ceccon, A. Gambaro, P. Ganis, S. Santi, A. Venzo, *Organometallics* **1995**, *14*, 2430–2434; h) E. V. Mutseneck, P. V. Petrovskii, A. R. Kudinov, *Russ. Chem. Bull.* **2004**, *53*, 2090–2091.

[4] For *syn*-μ-indenyl bimetallic complexes, see: a) K. Jonas, W. Rüsseler, K. Angermund, C. Krüger, E. Raabe, *Angew. Chem.* **1986**, *98*, 905-906; *Angew. Chem. Int. Ed. Engl.* **1986**, *25*, 928–929; b) F. Gauvin, B. James, S. Edmond, J. F. Harrod, *J. Am. Chem. Soc.* **1992**, *114*, 1489–1491; c) C. Bonifaci, A. Ceccon, A. Gambaro, P. Ganis, S. Santi, G. Valle, A. Venzo, *Organometallics* **1993**, *12*, 4211–4214; d) C. Bonifaci, A. Ceccon, A. Gambaro, P. Ganis, S. Santi, G. Valle, A. Venzo, *J. Organomet. Chem.* **1995**, *492*, 35–39; e) P. Cecchetto, A. Ceccon, A. Gambaro, S. Santi, *Organometallics* **1998**, *17*, 752–762; f) S. Sun, C. A. Dullaghan, G. B. Carpenter, A. L. Rieger, P. H. Rieger, D. A. Sweigart, *Angew. Chem.* **1995**, *107*, 2734-2737; *Angew. Chem. Int. Ed. Engl.* **1995**, *34*, 2540–2542; g) A. A. Trifonov, E. A. Fedorova, G. K. Fukin, E. V. Baranov, N. O. Druzhkov, M. N. Bochkarev, *Chem. Eur. J.* **2006**, *12*, 2752–2757; h) R. Gyepes, I. Cisarova, M. Horacek, J. Cejka, L. Petrusova, K. Mach, *Collect. Czech. Chem. Commun.* **2000**, *65*, 1248–1261; i) J. A. Cabeza, I. del Río, J. M. Fernández-Colinas, P. García-Álvarez, D. Miguel, *Organometallics* **2007**, *26*, 1414–1423.

[5] For μ^3-η^5:η^2:η^2-bonding mode, see: a) A. Eisenstadt, F. Frolow, A. Efraty, *J. Chem. Soc., Chem. Commun.* **1982**, 642–643; b) H. Chen, P. R. Raithby, G. N. Ward, *J. Chem. Soc., Chem. Commun.* **1995**, 755–756; c) M. I. Bruce, B. W. Skelton, A. H. White, N. N. Zaitseva, *Inorg. Chem. Commun.* **1999**, *2*, 17–20; d) P. Schooler, B. F. G. Johnson, L. Scaccianoce, H. Hopf, *J. Chem. Soc., Dalton Trans.* **2000**, 199–204; e) M. I. Bruce, B. W. Skelton, A. H. White, N. N. Zaitseva, *J. Cluster. Sci.* **2002**, *13*, 235–247; f) D. Chen, B. Mu, S. Xu, B. Wang, *J. Organomet. Chem.* **2006**, *691*, 3823–3833; g) Y. L. K. Tan, W. K. Leong, *J. Organomet. Chem.* **2007**, *692*, 768–773.

[6] For other new coordination modes, see: a) R. Khayatpoor, J. R. Shapley, *Organometallics* **2000**, *19*, 2382–2388; b) M. J. Calhorda, C. C. Romão, L. F. Veiros, *Chem. Eur. J.* **2002**, *8*, 868–875; c) C. A. Bradley, E. Lobkovsky, P. J. Chirik, *J. Am. Chem. Soc.* **2003**, *125*, 8110–8111; d) C. A. Bradley, I. Keresztes, E. Lobkovsky, V. G. Young, P. J. Chirik, *J. Am. Chem. Soc.* **2004**, *126*, 16937–16950; e) C. A. Bradley, E. Lobkovsky, P. J. Chirik, *J. Am. Chem. Soc.* **2005**, *127*, 10291–10304; f) L. F. Veiros, *Chem. Eur. J.* **2005**, *11*, 2505–2518; g) C. A. Bradley, E. Lobkovsky, I. Keresztes, P. J. Chirik, *J. Am. Chem. Soc.* **2006**, *128*, 6454–6467; h) C. Sui-Seng, G. D. Enright, D. Zargarian, *J. Am. Chem. Soc.* **2006**, *128*, 6508–6519; i) C. A. Bradley, L. F. Veiros, D. Pun, E. Lobkovsky, I. Keresztes, P. J. Chirik, *J. Am. Chem. Soc.* **2006**, *128*, 16600–16612; j) C. A. Bradley, I. Keresztes, E. Lobkovsky, P. J. Chirik, *Organometallics* **2006**, *25*, 2080–2089; k) L. F. Veiros, *Organometallics* **2006**, *25*, 2266–2273; l) S. Wang, X. Tang, A. Vega, J.-Y. Saillard, E. Sheng, G. Yang, S. Zhou, Z. Huang, *Organometallics* **2006**, *25*, 2399–2401.

[7] a) P. Jutzi, U. Siemeling, *J. Organomet. Chem.* **1995**, *500*, 175–185; b) P. Jutzi, T. Redeker, *Eur. J. Inorg. Chem.* **1998**, 663–674; c) C. Müller, D. Vos, P. Jutzi, *J. Organomet. Chem.* **2000**, *600*, 127; d) U. Siemeling, *Chem. Rev.* **2000**, *100*, 1495–1526; e) H. Butenschon, *Chem. Rev.* **2000**, *100*, 1527–1564; f) P. J. Fischer, K. M. Krohn, E. T. Mwenda, V. G. Young Jr., *Organometallics* **2005**, *24*, 1776–1779.

[8] D. Chen, Y. Li, B. Wang, S. Xu, H. Song, *Organometallics* **2006**, *25*, 307–310.

[9] H. Zhang, J. Ma, Y. L. Qian, J. L. Huang, *Organometallics* **2004**, *23*, 5681–5688.

[10] D. Braga, F. Grepioni, E. Parisini, P. J. Dyson, A. J. Blake, B. F. G. Johnson, *J. Chem. Soc., Dalton Trans.* **1993**, 2951–2957.

[11] a) B. K. Teo, G. Longoni, F. R. K. Chung, *Inorg. Chem.* **1984**, *23*, 1257–1266; b) D. Michael, P. Mingos, *Acc. Chem. Res.* **1984**, *17*, 311–319.

[12] a) D. Wang, H. Shen, M. G. Richmond, M. Schwartz, *Organometallics* **1995**, *14*, 3636–3640; b) R. Pattacini, G. Predieri, A. Tiripicchio, C. Mealli, A. D. Phillips, *Chem. Commun.* **2006**, 1527–1529; c) D. Belletti, P. Braunstein, A. Messaoudi, R. Pattacini, G. Predieri, A. Tiripicchio, *Chem. Commun.* **2007**, 141–143.

[13] J. F. Corrigan, M. Dinardo, S. Doherty, G. Hogarth, Y. Sun, N. J. Taylor, A. J. Carty, *Organometallics* **1994**, *13*, 3572–3580.

[14] A. Eisenstadt, C. M. Giandomenico, M. F. Frederick, R. M. Laine, *Organometallics* **1985**, *4*, 2033–2039.

[15] a) J. Lin, B. Wang, S. Xu, H. Song, *J. Organomet. Chem.* **2006**, *691*, 2528–2533; b) R. Khayatpoor, J. R. Shapley, *Organometallics* **2002**, *21*, 4794–4798.

[16] V. S. Sridevi, W. K. Leong, *J. Organomet. Chem.* **2007**, *692*, 4909–4916.

[17] Z. Ziniuk, I. Goldberg, M. Kol, *J. Organomet. Chem.* **1997**, *545–546*, 441–446.

[18] For recent papers on the chemistry of double-bond migration, see: a) S. Krompiec, N. Kuźnik, M. Krompiec, R. Penczek, J. Mrzigod, A. Tórz, *J. Mol. Catal. A Chem.* **2006**, *253*, 132–146; b) N. Kuźnik, S. Krompiec, *Coord. Chem. Rev.* **2007**, *251*, 222–233.

[19] a) H. Chen, B. F. G. Johnson, J. Lewis, P. R. Raithby, *J. Chem. Soc., Chem. Commun.* **1990**, 373–374; b) H. Chen, M. Fajardo, B. F. G. Johnson, J. Lewis, P. R. Raithby, *J. Organomet. Chem.* **1990**, *389*, C16–C18.

[20] a) P. F. Jackson, B. F. G. Johnson, J. Lewis, M. McPartlin, W. J. H. Nelson, *J. Chem. Soc., Chem. Commun.* **1979**, 735–736; b) C. R. Eady, P. F. Jackson, B. F. G. Johnson, J. Lewis, M. C. Malatesta, *J. Chem. Soc., Dalton Trans.* **1980**, 383–392.

[21] E. V. Dehmlow, C. Bollmann, *Tetrahedron Lett.* **1991**, *32*, 5773–5776.

Received: November 6, 2007
Published Online: February 27, 2008

